Mathematical Modeling of Rhesus Cytomegalovirus (RhCMV) Placental Transmission in Seronegative Rhesus Macaques

Yishu Gong[1], Matilda Moström[2], Claire Otero[3], Sarah Valencia[4] Amitinder Kaur[2], Sallie R. Permar[5], Cliburn Chan*[6,7]

1 Department of Mathematics, Duke University, Durham, NC, USA
2 Department of Immunology, Tulane National Primate Research Center, Covington, LA, USA
3 Department of Pathology, Duke University, Durham, NC, USA
4 Duke Human Vaccine Institute, Duke University Medical Center, Durham, NC, USA
5 Department of Pediatrics, Joan & Weill Cornell Medicine, New York City, NY, USA
6 Department of Biostatistics and Bioinformatics, Duke University, Durham, NC, USA
7 Center for Human Systems Immunology, Duke University, Durham, NC, USA

* ccliburn.chan@duke.edu

Abstract

Approximately 1 in 200 infants is born with congenital cytomegalovirus (CMV), making it the most common congenital infection. About 1 in 5 congenitally-infected babies will suffer long-term sequelae, including sensorineural deafness, intellectual disability, and epilepsy. CMV infection is highly species-dependent, and the Rhesus CMV (RhCMV) infection of rhesus monkey fetuses is the only animal model that replicates essential features of congenital CMV infection in humans, including placental transmission, fetal disease, and fetal loss. To better understand the determinants and dynamics of congenital CMV transmission, we developed a mathematical model for placental transmission, comprising of maternal, placental, and fetal compartments using parameters from literature and experimental data from RhCMV seronegative rhesus macaques inoculated with RhCMV at 7.7-9.0 weeks of pregnancy. The model was then used to study the effect of the timing of inoculation, maternal immune suppression, and hyper-immune globulin infusion on the risk of placental transmission in the context of primary and reactivated chronic maternal CMV infection.

Author summary

Congenital cytomegalovirus (CMV) is the most common congenital infection in humans. Congenial CMV affects 1 in 200 infants, and can result in sensorineural deafness, intellectual disability, epilepsy, and death. The Rhesus CMV (RhCMV) model is the only animal model that replicates essential features of congenital CMV infection and fetal sequelae in humans and provides a critical experimental system to develop mechanistic insight. We propose a novel mathematical model for CMV transmission that integrates viral dynamics in the maternal, placental, and fetal compartments. We calibrate the model using data from RhCMV transmission experiments and show that the model can recapitulate experimental observations of primary versus reactivated chronic CMV infection in pregnancy, primary infection at different stages in pregnancy,

and infection in the presence of varying degrees of immune suppression and hyper-immune globulin infusion. Our *in-silico* model provides a means to rapidly explore mechanistic hypotheses for the physical, viral, and immune determinants of CMV transmission to complement and support expensive and difficult experiments on non-human primates.

Introduction

Cytomegalovirus, or CMV, is the causative agent for of the most common human congenital infection and can result in multiple long-term deficits in infants, especially neurological defects and hearing loss. Congenital CMV occurs in 0.7% of all pregnancies [1] and is the main cause of non-genetic hearing loss, permanent sensory nerve and neurocognitive impairment in infants worldwide. Primary infection with CMV during pregnancy can result in transmission rates above 30%, but the transmission rate of congenital CMV is less than 2% among mothers with reactivated chronic infection. Species-specific CMV infections results in species-specific pathology, and only non-human primate (NHP) CMV models have recapitulated the neurological deficits seen in congenital human CMV infections [2]. This model has been used to demonstrate the importance of maternal CD4+ T cell and pre-existing antibodies in prevention of fetal transmission and disease [2, 3]. The need to use experimental NHP models such as the Rhesus CMV macaque (Macaca mulatta) to perform relevant proof-of-concept studies of the determinants of congenital CMV transmission and disease poses a major challenge to understanding and developing effective therapies to prevent this disease.

There have only been a limited number of previously published work on the mathematical modeling of CMV infection. Kepler et al developed a system of ordinary differential equations (ODE) to model CMV infection or reactivation in solid organ transplant recipients who are given immunosuppressive therapy [4]. The paper focused on the effect of the level of immune suppression on the viral load. Bryan et al developed several deterministic model of the cytolytic immune pressure during primary CMV infection to predict the dynamics of oral shedding [5], as well as a stochastic model to simulate early stages CMV infections in infants.

However, none of these previous studies directly model the process of CMV transmission from the maternal blood across the placenta to the fetus, which we believe is essential for simulating therapeutic interventions to prevent congenital infection. In this paper, we develop a mathematical model for CMV transmission that encompasses host-virus dynamics in the mother, placenta, and fetus. This model allows us to explore the interaction of immune control of virus in the mother, virus clearance in the placenta, placental growth, and immune interventions (CD4+ T cell depletion or hyperimmune globulin therapy) to predict the number of transmitted viruses, timing of infection, and overall risk of congenital infection in the fetus. Such a model can help the future design of human CMV (HCMV) studies based on small NHP intervention experiments, while minimizing the use of resource intensive NHPs.

Materials and methods

Experimental procedure

The model was calibrated using data from primary RhCMV infection of seronegative Rhesus macaque dams [2, 3]. In these experiments, twelve pregnant RhCMV seronegative rhesus macaques were assigned to an immunocompetent group (n=3) or an immune-suppressed group (n=9). The immune-suppressed group was depleted of their CD4+ T cell via anti-CD4 monoclonal antibody infusion prior to inoculation. Both

groups of macaques were inoculated with RhCMV at 7.7-9.0 weeks of pregnancy, and RhCMV viral loads in maternal plasma and fetal amniotic fluid were measured longitudinally using quantitative PCR. We consider transmission to occur when fetal amniotic fluid was PCR-positive. Two of three of the immunocompetent group animals had detectable RhCMV DNA in amniotic fluid [2]. All 9 CD4+ T cell depleted animals had detectable RhCMV DNA in amniotic fluid, indicating 100% placental transmission [2,3]. The experimental measurements are presented in Fig. 1. All procedures involving animals were reviewed and approved by the Institutional Animal Care and Use Committee of Weill Cornell Medicine under IACUC protocol numbers: #0179-21 & #0180-21. No human subjects or field research was conducted.

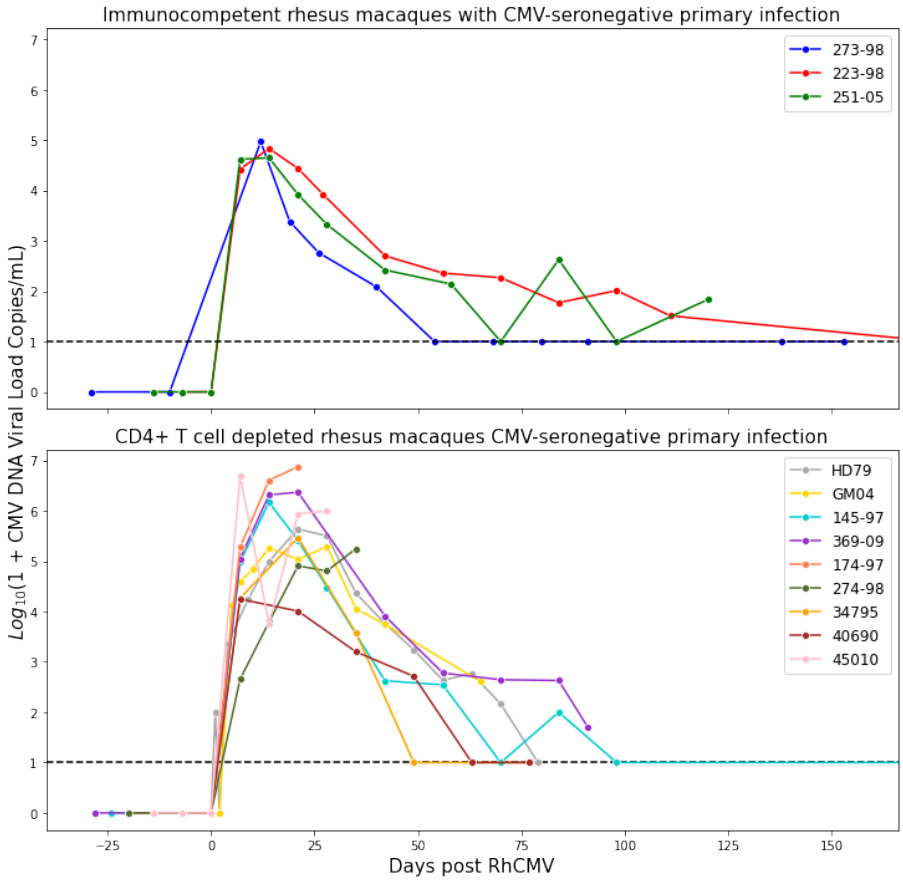

Fig 1. Plasma CMV viral loads in two groups of infected rhesus macaques (immunocompetent and CD4+ T cell depleted). Dashed lines represent the lower limit of detection (LOD).

Model Structure

Maternal compartment

To model immune and viral dynamics in the mother, we use a model originally developed for CMV infection in kidney transplant recipients on immune suppression [4]. This model builds on the standard virus dynamics model [6], with an additional term regulating the degree of immune suppression. The model structure is shown in Figure 2,

and can be written as a system of ordinary differential equations (ODE):

$$\begin{aligned} dV/dt &= n\delta R_I - cV - fkR_S V, \\ dE/dt &= (1-\epsilon_S)\left(\lambda_E\left(1-\frac{E}{e}\right)E + \rho V\right), \\ dR_I/dt &= kR_S V - \delta R_I - (1-\epsilon_S)mER_I + \alpha_0 R_L - \kappa R_I, \\ dR_S/dt &= \lambda\left(1-\frac{R_S}{r_S}\right)R_S - kR_S V, \\ dR_L/dt &= \lambda\left(1-\frac{R_L}{r_L}\right)R_L + \kappa R_I. \end{aligned} \tag{1}$$

In the ODE system (1), V denotes viral load (free virus) per μl-blood, E denotes virus-specific immune effector cells per μl-blood, R_I, R_S, and R_L denotes actively infected, susceptible cells, and latently infected cells per μl-blood respectively. A description of all model parameters is given in Table. 1.

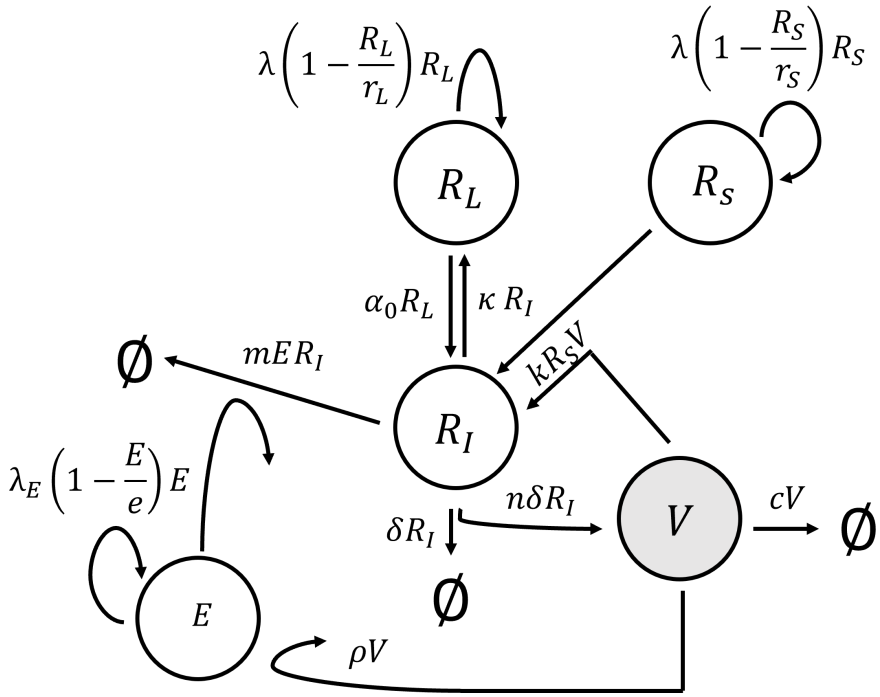

Fig 2. Schematic diagram of key processes in model of HCMV infection: infection $V + R_S \to R_I$, immune-induced cell lysis of infected cells $E + R_I \to E + \emptyset$, spontaneous reactivation from latency $R_L \to R_I$, establishment of latency $R_I \to R_L$, viral induced cell lysis $R_I \to nV$, viral clearance $V \to \emptyset$, and maintenance of cell populations (arching arrows).

Placental compartment

We model the transmission of CMV through the placenta as a diffusion process with decay. While physical diffusion is an unrealistic physical model for CMV in the placenta, we treat this as a phenomenological representation intended to capture the coarse grain dynamics of placental transmission. Similar PDE models have been shown to accurately capture the dynamics of HIV passage across the urogenital mucus epithelium [7]. For

simplicity, we assume homogeneous dynamics in the radial directions and model diffusion through the placental depth-wise as a 1D diffusion process, from maternal blood lake to the fetal circulation. This gives:

$$\frac{\partial Q}{\partial t} = D\frac{\partial Q^2}{\partial x^2} - \mu Q. \tag{2}$$

with boundary conditions:

$$Q = 0, \quad x = 0, \quad t \geq 0, \tag{3}$$

$$Q = V(t), \quad x = l, \quad t \geq 0, \tag{4}$$

and initial condition:

$$Q = 0, \quad 0 < x < l, \quad t = 0. \tag{5}$$

Here, Q denotes the concentration of CMV. Constant D denotes the diffusion coefficient. Constant μ denotes the death rate of the CMV. The boundary conditions assume that the virus concentration at the maternal-placental interface is the same as the viral concentration in maternal blood, and that once a virus crosses the placenta into the fetus, it is carried away rapidly by the fetal blood flow.

With simplified versions of these boundary conditions (e.g., maternal viral concentration is constant or can be approximated by a simple polynomial, (2) - (5) can be solved analytically using Fourier series to obtain a closed form solution (See S1 File in Supplementary Materials). This analytic solution is used to verify the correctness of numerical simulations needed for more complex maternal viral load dynamics.

The number of viruses that enter the infant, denoted by C,is estimated by:

$$C = \int_0^T D\frac{\partial Q}{\partial x}\bigg|_{x=0} G(t)dt, \tag{6}$$

where $G(t)$ refers to the growth curve of placenta throughout pregnancy. Here we assume that $G(t)$ has the form of a logistic curve in the range where we have data points, and has a linear expression that connects to the origin:

$$G(t) = \begin{cases} \frac{a}{1+e^{-(b(t-c))}}, \text{if } t \geq 40; \\ g \cdot t, \text{if } 0 \geq t \leq 40 \end{cases} \tag{7}$$

By treating the viral flux

$$\lambda(t) := D\frac{\partial Q}{\partial x}(0,t)G(t) \tag{8}$$

as the rate for an inhomogeneous Poisson point process, we can obtain the time that each virus arrives in the fetal compartment.

Fetal compartment

We model the arrival and subsequent fate of each CMV virion that arrives in the fetus using a stochastic process to accurately reflect the dynamics of small populations. Since we only model the early infection dynamics in the fetus, we assume that the number of susceptible cells is constant. Once the virus enters a susceptible cell, we consider two stochastic models for the subsequent dynamics, with and without latent viral infection stages, respectively:

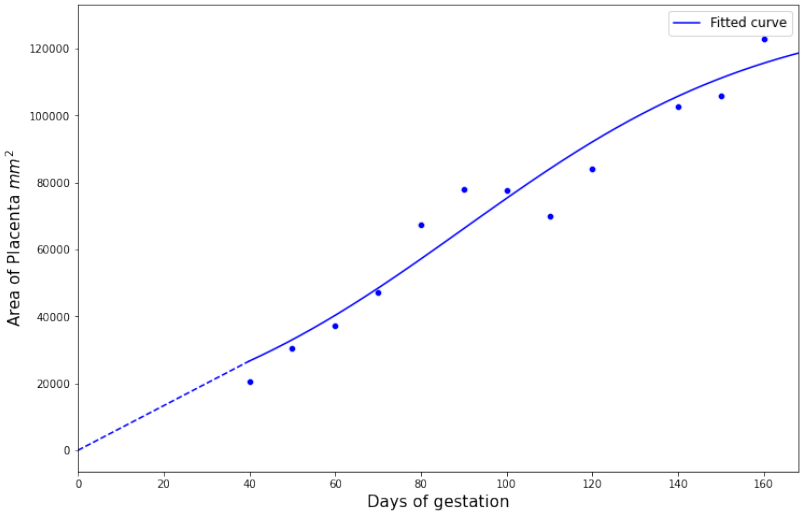

Fig 3. Growth function $G(t)$ for placenta surface area over time. Using data from [8], the area of the placenta of fetal rhesus macaques, from the fortieth day of gestation to term were plotted and fitted using a logistic curve. Note that the dashed line is a linear interpolation between the predicted value at the first available data point and the origin since a logistic curve cannot pass the origin.

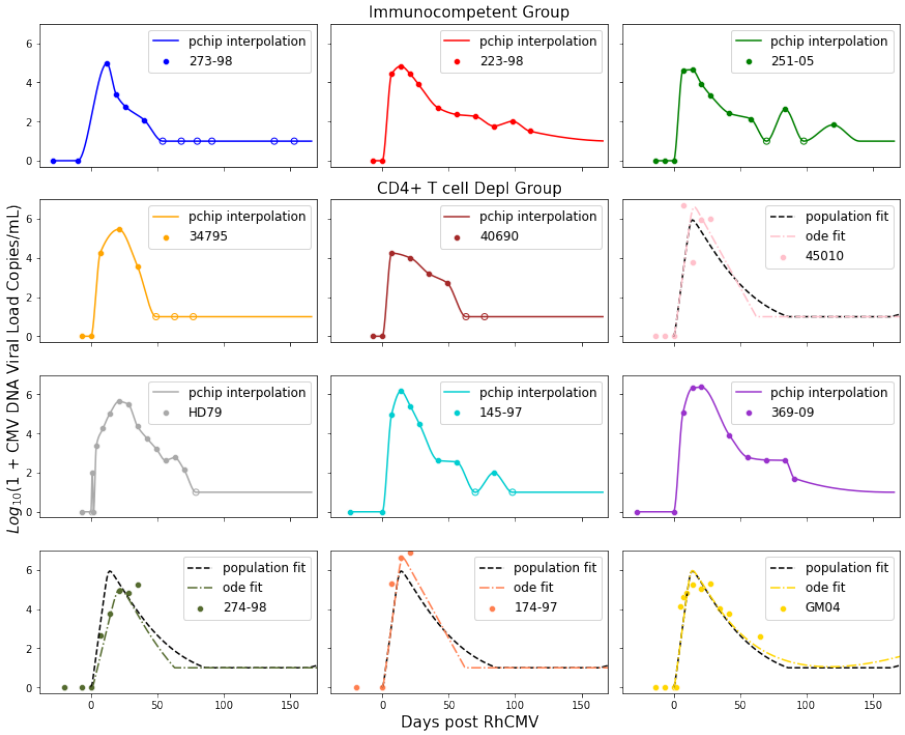

Fig 4. Interpolation and ODE fits for RhCMV seronegative rhesus macaque dams following primary RhCMV infection. The first two rows are the immunocompetent group; dashed black line is the population fit. The bottom two rows are the CD4+ T cell depleted dam group; dashed line is the population fit. Open circles refer to limit of detection (LOD) and specified as left censored ranges in Monolix.

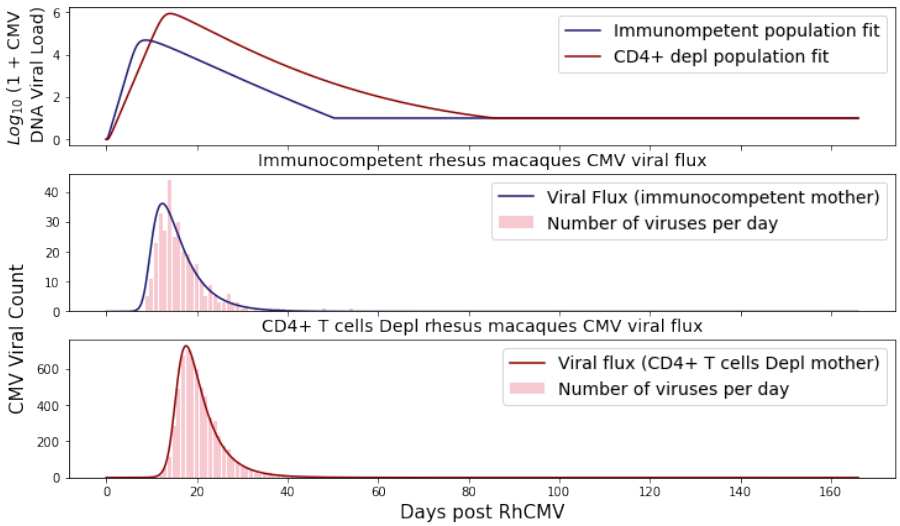

Fig 5. Inhomogeneous Poisson sampling from the viral flux. The maternal dynamics comes from the population fits of immunocompetent and CD4+ T cell depleted groups of rhesus macaques. We have used different transplacental scales for the y-axis to show the daily viral counts clearly – note that the difference of CMV viral load between immunocompetent and CD4+ T cell depleted dam groups is more than one order of magnitude.

Model 1: Susceptible cell with latent stage:

$$\begin{aligned} S + V \to L \quad &\text{with} \quad c_1 = \beta SV, \\ L \to \phi \quad &\text{with} \quad c_2 = d, \\ L \to I \quad &\text{with} \quad c_3 = \alpha, \\ I \to \phi \quad &\text{with} \quad c_4 = d, \\ I \to I + V \quad &\text{with} \quad c_5 = \omega, \\ V \to \phi \quad &\text{with} \quad c_6 = \gamma. \end{aligned} \tag{9}$$

Model 1 corresponds to a target-cell limitation model given in [5], which has a reproductive number R_0 given by:

$$R_0 = \frac{\beta S_0 \omega}{cd(1 + \frac{\gamma}{\alpha})} = 1.02. \tag{10}$$

Model 2: Susceptible cell without latent stage:

$$\begin{aligned} S + V \to I \quad &\text{with} \quad c_1 = \beta SV, \\ I \to \phi \quad &\text{with} \quad c_2 = d, \\ I \to I + V \quad &\text{with} \quad c_3 = \omega, \\ V \to \phi \quad &\text{with} \quad c_4 = \gamma. \end{aligned} \tag{11}$$

Model 2 corresponds to a target infectiion virus model given in [9], which has a reproductive number R_0 given by:

$$R_0 = \frac{\beta S_0 \omega}{cd(1 + \frac{\beta S_0}{c})} = 1.25. \tag{12}$$

For each virion, we choose between Model 1 and 2 as follows: Assuming that the ratio between the susceptible cells that go through latent stage and the susceptible cells that

become infected cells is $r : (1 - r)$, we draw a uniform random variable s between 0 and 1, and if $s < r$, we run model 1 given by Equation (9), else if $s > r$, we run model 2 given by (11) (In our sample runs, we use $r = 0.5$). Since we assume that the number of susceptible cells remains constant over the period of interest, we do not allow the production and death of susceptible cells, i.e., $S = S_0$ and then $\beta S = \beta S_0$ is a constant 0.0012 (virions $\cdot$ day)$^{-1}$.

Model calibration

Maternal compartment

We used the parameters for human CMV infection given in Kepler et al [4] as initial guesses, we kept t_H (Half-life of virions), $\tilde{E}$ (Equilibrium level of CMV-specific effector cells), and $\tilde{V}$ (Equilibrium level of virions) fixed. When we perform parameter estimation for immunocompetent rhesus macaques, we set ϵ_S (Level of immune suppression) to be 0.

The remaining parameters for the ODE system were estimated using nonlinear mixed effects regression, as implemented in the Monolix software (version 2020R2, Lixoft) [10]. Monolix uses Stochastic Approximation Expectation Maximization (SAEM) to perform parameter estimation [11], and can accommodate the use of viral loads below the limit of detection (left censoring). Population parameter estimates for both the control and immune suppressed grouped described by ODE system Equation (1) are summarized in Table. 1.

Placental compartment

We first estimate the growth curve for the placenta given by Equation (7). Using the data from [8] for pregnant rhesus macaques, we fitted a logistic function to obtain Fig. 3 with $a = 132434$, $b = 0.028$, $c = 90$ $g = 666.93$.

For boundary conditions on the maternal-placental interface, we need to estimate a continuous function from discrete experimental measures of viral load over time. Where there are sufficient data points, we fit the experimental measures directly using Piecewise Cubic Hermite Interpolating Polynomial (PCHIP) interpolation [12]. Unlike the more commonly used cubic spline interpolation, PCHIP avoids overshoots and can accurately connect the flat regions without creating artificial oscillations. For rhesus macaques with insufficient data points, we use the ODE model proposed by [4] to obtain a smooth trajectory for each animal, as well as population fits for immunocompetent and CD4+ T cell depleted dam groups using a nonlinear mixed effect model. These fits are shown in Fig. 4.

For the PDE Equation (2), we used the diffusion coefficient of HIV through stroma as our D [7]. We observe from the experimental data that all fetal infections occurred within 2-4 weeks after the mothers are infected with RhCMV. Using this, we can approximate the distance l that the virus needs to travel. The diffusion coefficient determines the time it takes a solute to diffuse a given distance in a medium:

$$t \approx \frac{l^2}{2 \cdot D}.$$

Then we have:

$$l \approx \sqrt{2 \cdot t \cdot D} \approx 0.6 \ mm.$$

We can also calibrate μ in (2) using the experimental data so that the probability of transplacental RhCMV transmission for immunocompetent rhesus macaques using stochastic simulation is between 30% to 40%, and we obtain $\mu = 1$ (day)$^{-1}$.

Fetal compartment

For the stochastic simulation of the fate of CMV arrivals in the fetus given by Equations (9) and (11), all parameters are from [5] and [13]. These parameters are shown in Table 2.

With the arrival time of each virus, we run the Gillespie algorithm [14] to simulate viral dynamics in the fetus, and define a fetus as infected once the viral load exceeds a prespecified threshold. Repeated runs of simulations then yield a distribution for the time of infection and the probability of transplacental transmission. Fig. 5 shows the viral flux functions and simulated arrival times corresponding to population fits of immunocompetent and CD4+ T cell depleted rhesus macaques.

Results

Probability of trans-placental transmission

Since viruses arriving in the fetus may be cleared without leading to sustained infection, we define transplacental transmission to have occurred when more than $M = 800$ copies of RhCMV are in the fetus at a given time, and define the time from maternal inoculation with virus to this event as the time to transmission. About the 100th day of 155 gestation, all the congenital infections including reactivated chronic infections would be expected to have happened [2]. At this time, fetal weight is measured to be around 0.14 kg [8]. Using the blood volume of rhesus macaques at 60 mL/kg [15], we can calculate the fetus has $\approx 8.4mL$ blood in total. Since the limit of detection of CMV is 100 copies/ml [2], we calculated the threshold M, total number of viruses in fetus, to be around 800 copies.

While the threshold is arbitrary, our simulations show that once this threshold is crossed, spontaneous clearance of virus is extremely unlikely. We first estimate the probability p that a single replicating virus that passes through the placenta will lead to sustained infection. In fact, theoretically, we can obtain the extinction probability when we start with one virus using a continuous time branching process. This means the probability of any number of viruses surviving is $\frac{d(R_0-1)}{\omega}$ with target infection virus model derived in [16] and with R_0 given by Equation (12). However, we consider there is sustained infection only if the number of viruses is above a threshold. Therefore, we run stochastic simulations to directly estimate the value of p. Using stochastic simulation is more realistic since we can estimate the probability of viruses count reaching a specified threshold value M, as well as incorporate the switching between models with (Equations (9)) and without (Equations (11)) latent stages. With initial values $S_0 = 4 \cdot 10^8, L_0 = 0, I_0 = 0, V_0 = 1$, we run Gillespie algorithm 10^6 times with two stopping criteria:

1. No more viruses, latent cell, or infected cells are left (no persistent infection);
2. Viruses count has reached M copies (persistent infection).

Then, if we consider that every virus can cause persistent infection independently, we can estimate on the probability of infection if N viruses travel through the placenta as:

$$P = 1 - (1 - p)^N. \tag{13}$$

As a result, we can obtain a cumulative probability over time since we can calculate the number of viruses using (8):

$$P(t) = 1 - (1 - p)^{N(t)}, \; N(t) = \int_0^t \lambda(\tau) d\tau. \tag{14}$$

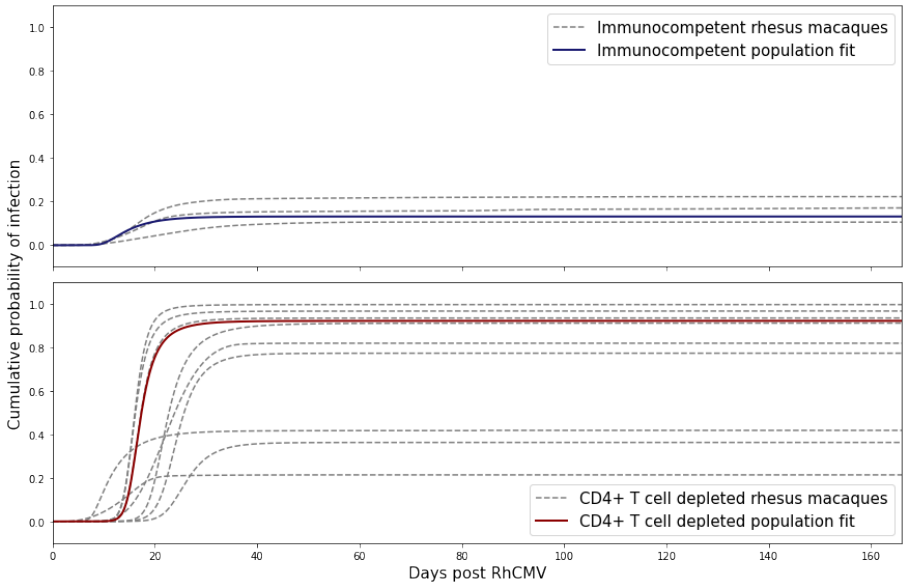

Fig 6. Probability of transplacental transmission of RhCMV following primary infection of immunocompetent and CD4+ T cell depleted dams. The blue line refers to the result using the immunocompetent dam population fit as maternal viral dynamics. The gray dashed line represents each individual immunocompetent rhesus macaques. The red line refers to the result using the CD4+ T cell depleted macaque dam population fit to the ODEs for maternal viral dynamics. The gray dashed-dotted line refers to each individual CD4+ T cell depleted rhesus macaques. Graph generated taking $M = 800$ copies and (13).

This is a heuristic estimate since there can be multiple viruses that enter the fetus around the same time, which could increase the probability of infection.

Primary and reactivated chronic maternal RhCMV infections

We simulate reactivated chronic maternal RhCMV infection by running (1) for an extended period until the viral dynamics approach equilibrium. We can then compare the transmission probabilities between primary and reactivated chronic infections in Fig. 9. For both immunocompetent and CD4+ T cell depleted rhesus macaques, the risk of congenital CMV following primary maternal infection is much higher than that following reactivated chronic infection.

Immune suppression increase likelihood of placental transmission

As explained in [2], maternal CD4+ T cell plays a crucial role against severe congenital CMV disease in their nonhuman primate model of placental CMV transmission. Moreover, [17] demonstrated the importance of the maternal CD4+ T cell responses in human. Our model echoes this study and shows that level of immune suppression level in general strongly influences the probability of transplacental transmission. From experimental 188 data, we observe that the CD4+ T cell depleted group of rhesus macaque dams have much higher plasma viral load. Therefore, we observe more virus entering the infant during pregnancy. As expected, we observe much higher

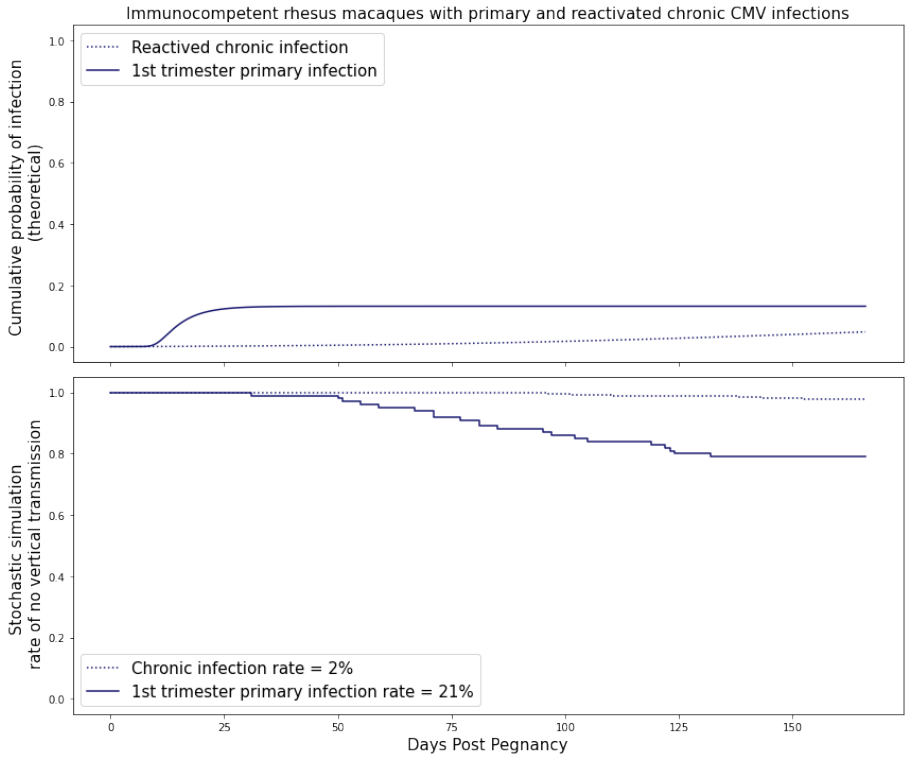

Fig 7. Probability of transplacental transmission of reactivated chronic RhCMV infections during different trimesters of pregnancy. The maternal dynamics comes from the equilibrium values of the population fits of immunocompetent groups of rhesus macaques. Graph generated taking threshold $M = 800$ copies. The blue dashed line refers to immunocompetent mothers with reactivated chronic infection. The blue solid line refers to immunocompetent mothers that is infected during the first trimester of pregnancy.

probabilities of transplacental transmission for CD4+ T cell depleted dam group. In Fig. 6, we can see that our calibrated model predicts that the probability of RhCMV infection for immunocompetent rhesus macaque dams is 12%, and the probability of RhCMV infection for CD4+ T cell depleted rhesus macaque dams is 90%.

Inoculation in different trimesters

In humans, it has been observed that the risk of congenital CMV following primary infection is 30-40% in the first and second trimesters, but rises to 40-70% in the third trimester [18]. We observe this same phenomenon in our model when we shift the time of viral inoculation from $t = 0$, $t = 55$ and $t = 110$ days, corresponding to first, second and third trimester infections in the Rhesus macaque model, which has an average gestation period of 166 days [8]. The model suggests that most, if not all, of the increase in risk with later trimesters can be attributed to the growth of the placenta inducing a larger viral flux on the placenta-fetus boundary, and a correspondingly higher probability of trans-placental transmission as shown in Fig. 9 and Fig. 10. While we cannot rule out that changes in the immune milieu also play a role [19], the model provides a parsimonious explanation and a major contribution by placental growth that is obvious in hindsight.

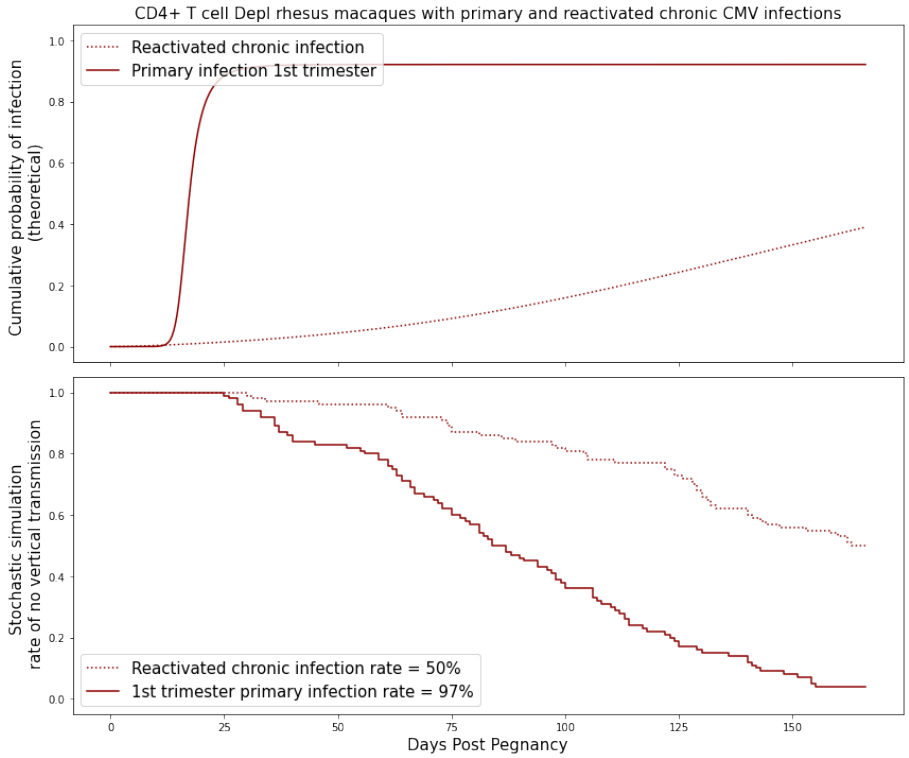

Fig 8. Probability of transplacental transmission of reactivated chronic maternal RhCMV infections during different trimesters of pregnancy. The maternal dynamics comes from the equilibrium values of the population fits of CD4+ T cell depleted rhesus macaques. Graph generated taking threshold $M = 800$ copies. The red dashed line refers to CD4+ T cell depleted dams with reactivated chronic infection. The red solid line refers to CD4+ T cell depleted mother that is infected during 1st trimester of pregnancy.

Prevention of Congenital Cytomegalovirus Infection with Hyperimmune Globulin following primary maternal infection

Postinfection Hyperimmune Globulin infusion was shown to reduce rates of placental HCMV transmission in several nonrandomized small-scale clinical trials [20, 21] and case-controlled studies [22, 23]. However, in a large-scale, randomized, placebo-controlled trial [24], the use of HIG after primary maternal CMV infection showed no efficacy. We can also extend (14) to evaluate the utility of HIG infusion at different times following primary maternal CMV infection at preventing congenital CMV infection:

$$P(t) = 1 - (1-p)^{N(t)},\ N(t) = \int_0^t \lambda(\tau) H(\tau) d\tau,$$
$$H(\tau) = \begin{cases} 1, \text{if } \tau < T_{\text{inj}} \\ (1 - \epsilon_{\text{eff}}), \text{if } T \geq T_{\text{inj}} \end{cases} \quad (15)$$

In the above equation, T_{inj} refers to the time of HIG injection, and ϵ_{eff} refers to the assumed effectiveness of HIG treatment. This simple model assumes that HIG maintains the same efficacy for all time, so overestimates the utility in the real world, where HIG concentrations in plasma would diminish over time. The reduction in predicted risk of fetal CMV infection with different time and effectiveness of HIG

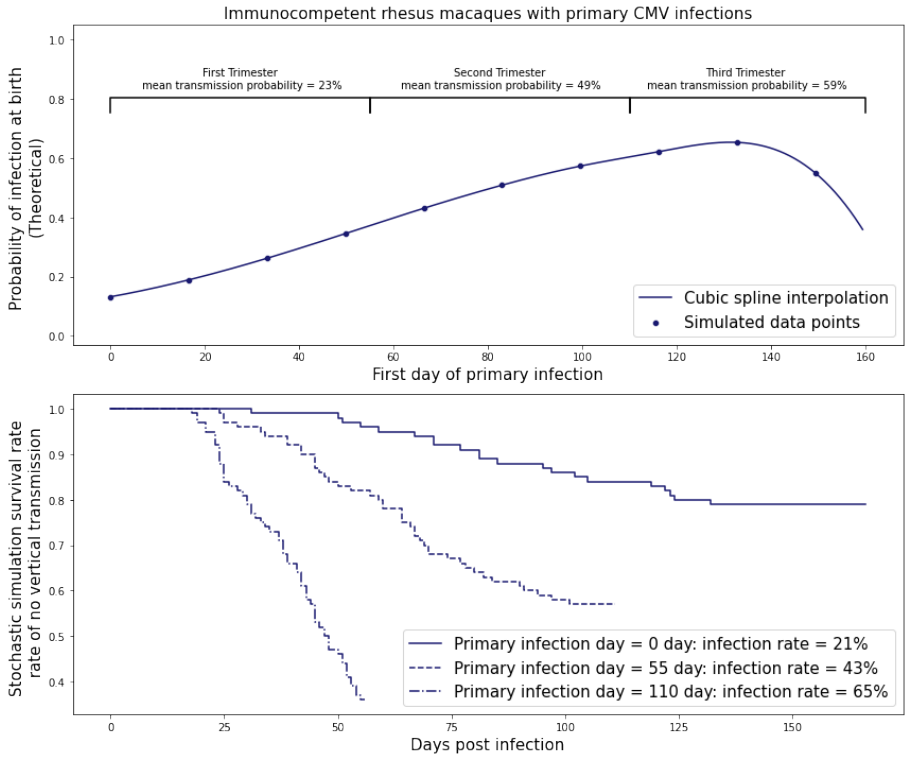

Fig 9. Probability of immunocompetent mothers transplacental transmission of primary RhCMV infections during different trimesters of pregnancy. The maternal dynamics comes from the population fits of immunocompetent group of rhesus macaques with starting time $t = 0$ day (Primary infection 1^{st} trimester), time $t = 55$ day (Primary infection 2^{nd} trimester), and $t = 110$ day (Primary infection 3^{rd} trimester). Graph generated taking threshold $M = 800$ copies.

infusion for immunocompetent and CD4+ T cell depleted immune suppressed hosts are shown in Tables. 3 and 4 respectively. Our simulations suggest that HIG infusion for immunocompetent hosts has little utility if given later than two weeks from maternal infection. As maternal CMV infection is frequently asymptomatic, diagnosis is dependent on seroconversion, which takes at least 2 weeks, indicating that HIG delivery based on serologic diagnosis serologic diagnosis may not be able to prevent transplacental CMV transmission.

Discussion

The determinants of congenital CMV transmission are challenging to study experimentally, as only the RhCMV NHP model recapitulates the features of human congenital CMV placental transmission and fetal neurologic disease. NHP experiments are extremely costly and time-consuming, and hence need to be designed to maximize the generation of new knowledge. The mathematical model for the placental transmission of CMV we describe here can serve as an *in silico* experimental system, facilitating the generation and identification of the most promising hypotheses for validation in RhCMV experiments.

Our mathematical model for placental transmission considers CMV dynamics in the

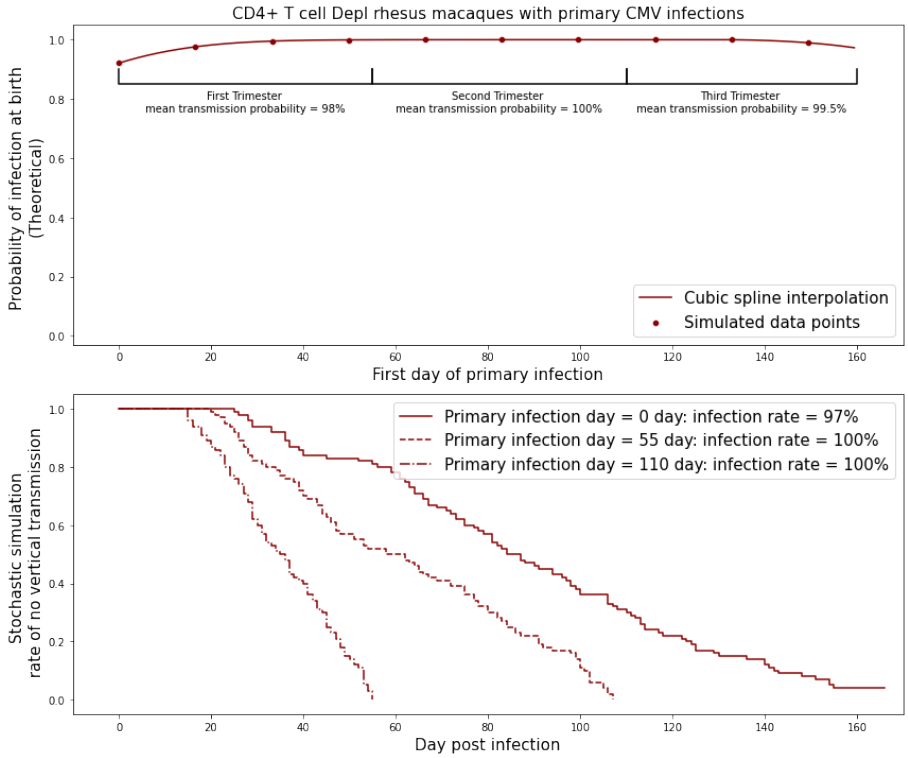

Fig 10. Probability of transplacental RhCMV transmission after primary maternal infections during different trimesters of pregnancy in CD4+ T cell depleted RhCMV seronegative dams. The maternal dynamics comes from the population fits of CD4+ T cell depleted rhesus macaque dams with starting time $t = 0$ day (Primary infection 1^{st} trimester), time $t = 55$ day (Primary infection 2^{nd} trimester), and $t = 110$ day (Primary infection 3^{rd} trimester). Graph generated taking threshold $M = 800$ copies.

mother, the placenta, and the fetus. Each of these three physical compartments has its own unique characteristics that require a different mathematical framework to adequately represent. We also describe how we link the dynamics across physical compartments by careful consideration of conditions at the boundaries. Finally, we consider the simple fact that the placenta is growing throughout pregnancy, and incorporate this growth curve into the model framework.

We then calibrated the model using data from RhCMV experiments that compared the risks of placental RhCMV transmission for immunocompetent and CD4+ T cell depleted hosts. These experiments collected longitudinal measurements of the viral load in maternal plasma and fetal amniotic fluid, allowing us to also estimate the time that transmission occurred in cases where the fetus was infected. Using the calibrated model, we then simulated the dynamics of placental RhCMV transmission under several scenarios, and compared the risks of transmission with reactivated chronic versus primary maternal infection, with primary infection at different stages of pregnancy, and with immune suppression or immune augmentation by HIG infusion following primary maternal infection. For each scenario, the model predicts the probability of infection, as well as the most likely time window for congenital infection to occur, and an estimate of the number of potential founder viruses that cross the placenta.

The mathematical model and the *in silico* simulation is, of course, a highly simplified representation of an incredibly complex biological system. However, we

believe that it captures the major determinants of RhCMV transmission and can recapitulate experimental and clinical observations. For example, the model predicts that the number of transmitted founder viruses is typically small, consistent with studies of viral genomics in infected fetuses [25]. The model also predicts that delayed infusion of HIG more than 2 weeks after primary maternal infection has little effect in preventing congenital CMV transmission among immunocompetent hosts, consistent with the negative results of a recent clinical trial [26] where expectant mothers infected before 23 weeks' gestation were given monthly HIG infusions starting from serologic diagnosis of primary CMV infection based on low avidity CMV-specific IgG responses, which take at least 2 weeks to develop. With better experimental data, the model can be extended to include more mechanistic hypotheses, for example, to model the effect of vaccination or specific immune mechanisms that serve as barriers to placental transmission that are currently represented by a simple linear decay. We believe that this model will serve as a foundation for more realistic mechanistic models that will be useful for understanding, developing, and de-risking clinical trials of interventions to prevent congenital CMV infection.

Table 1. ODE Model parameter estimates

Parameter	Description	Immunocompetent	CD4+ Depl	Units
ρ	Virion induced immune response	2	3	cells/(virions · day)
n	Productivity of infected cell	$6 \cdot 10^{1}$	$6 \cdot 10^{1}$	cells/μl-blood
δ	Rate of viral induced cell death	$7.8 \cdot 10^{-1}$	$1.4 \cdot 10^{-1}$	day^{-1}
c	Rate of viral clearance	$1.5 \cdot 10^{-1}$	$2.8 \cdot 10^{-1}$	day^{-1}
k	Infection rate constant	$2.6 \cdot 10^{-4}$	$4.5 \cdot 10^{-4}$	μl/(virions · day)
m	Immune induced cell lysis	$8.3 \cdot 10^{-2}$	$3.2 \cdot 10^{-3}$	μl/(cells · day)
α_0	Exit and reactivation rate for monocytes	$1.7 \cdot 10^{-2}$	$1 \cdot 10^{-1}$	μl/(cells · day)
κ	Rate of latency	$5.5 \cdot 10^{-1}$	$1.4 \cdot 10^{-3}$	μl/(cells · day)
λ_E	Homeostatic replenishment of immune cells	$3.1 \cdot 10^{-4}$	$4.5 \cdot 10^{-4}$	day^{-1}
λ	Cell replenishment rate	$1 \cdot 10^{-3}$	$7.1 \cdot 10^{-4}$	day^{-1}
e	CMV-specific effector cell term	18	4	cells/μl-blood
ϵ_S	Level of immune suppression	0	$7.9 \cdot 10^{-1}$	-
f	Number of infecting virions per cell	1.4	$1 \cdot 10^{-1}$	-
r_S	Equilibrium level of susceptible cells	$5 \cdot 10^{2}$	$6 \cdot 10^{2}$	cells/μl-blood
r_L	Equilibrium level of latenT cell	$4 \cdot 10^{-2}$	$7 \cdot 10^{-2}$	cells/μl-blood
t_H	Half-life of virions during antiviral treatment	2	2	days
t_D	Doubling time of the virions	11.5	1	days
$\tilde{E}$	Equilibrium level of CMV-specific effector cells	10	10	cells/μl-blood
$\tilde{V}$	Equilibrium level of virions	$2 \cdot 10^{-2}$	$2 \cdot 10^{-2}$	virions/μl-blood

Supporting information

S1 File. Analytical Solution to Diffusion Equation with Varying Boundary Condition.pdf

S2 File. Code for Monolix.txt

S3. File Matlab Code for simulations.

Table 2. Stochastic simulation parameter estimates

Parameter	Description	Value	Units
S_0	Initial susceptible cell population	$4 \cdot 10^8$	cells
L_0	Initial latently infected cell population	1	cells
I_0	Initial infected cell population	0	cells
V_0	Initial viral population	0	virions
γ	Death rate of susceptible cells	1/4.5	cells/day
β	Rate of new infected cell	$3 \cdot 10^{-12}$	1/(virions· cells· day)
α	Lag (days) between cell infection and viral growth	1	day
d	Death rate of infected cells	0.77	cells/day
ω	New viruses per infected cell per day	1600	1/(virions· day)
c	Natural decay of virus	2	virion/day

Table 3. Probability of transplacental transmission with HIG treatment for immunocompetent group

HIG infusion day T_{inj}	Effectiveness $\epsilon_{\text{eff}} = 100\%$	Effectiveness $\epsilon_{\text{eff}} = 75\%$	Effectiveness $\epsilon_{\text{eff}} = 50\%$
Not Treated	13.00%	13.00%	13.00%
Day 21	11.36%	11.82%	12.27%
Day 14	6.24%	8.05%	9.78%
Day 7	0.02%	3.48%	6.83%

Table 4. Probability of transplacental transmission with HIG treatment for CD4+ T cell depleted group

HIG infusion day T_{inj}	Effectiveness $\epsilon_{\text{eff}} = 100\%$	Effectiveness $\epsilon_{\text{eff}} = 75\%$	Effectiveness $\epsilon_{\text{eff}} = 50\%$
Not Treated	92.08%	92.08%	92.08%
Day 21	80.70%	84.60%	87.67%
Day 14	7.00%	49.71%	72.85%
Day 7	0.02%	46.90%	71.87%

Acknowledgments

YG and CC are partially supported by P30-AI064518-17 and R25-AI140495-04. The research and all authors are supported by P01-AI129859-04.

References

1. Dollard SC, Grosse SD, Ross DS. New estimates of the prevalence of neurological and sensory sequelae and mortality associated with congenital cytomegalovirus infection. Reviews in medical virology. 2007;17(5):355–363.

2. Bialas KM, Tanaka T, Tran D, Varner V, De La Rosa EC, Chiuppesi F, et al. Maternal CD4+ T cells protect against severe congenital cytomegalovirus disease in a novel nonhuman primate model of placental cytomegalovirus transmission. Proceedings of the National Academy of Sciences. 2015;112(44):13645–13650.

3. Nelson CS, Cruz DV, Tran D, Bialas KM, Stamper L, Wu H, et al. Preexisting antibodies can protect against congenital cytomegalovirus infection in monkeys. JCI insight. 2017;2(13).

4. Kepler GM, Banks HT, Davidian M, Rosenberg ES. A model for HCMV infection in immunosuppressed patients. Mathematical and computer modelling. 2009;49(7-8):1653–1663.

5. Mayer BT, Matrajt L, Casper C, Krantz EM, Corey L, Wald A, et al. Dynamics of persistent oral cytomegalovirus shedding during primary infection in Ugandan infants. The Journal of infectious diseases. 2016;214(11):1735–1743.

6. Funk GA, Gosert R, Hirsch HH. Viral dynamics in transplant patients: implications for disease. The Lancet infectious diseases. 2007;7(7):460–472.

7. Adrianzen D, Katz D. Modeling Probability of Infection and Its Alteration by Microbicides by Integrating HIV Transport and Infection Dynamics With Drug Transport & Action. In: AIDS Research and Human Retroviruses. vol. 34; 2018. p. 289–289.

8. Van Wagenen G, Catchpole H, Negri J, Butzko D. Growth of the fetus and placenta of the monkey (Macaca mulatta). American journal of physical anthropology. 1965;23(1):23–33.

9. Perelson AS. Modelling viral and immune system dynamics. Nature reviews immunology. 2002;2(1):28–36.

10. Lixoft S. Monolix version 2020R2. URL http://lixoft com/products/monolix. 2018;.

11. Delyon B, Lavielle M, Moulines E. Convergence of a stochastic approximation version of the EM algorithm. Annals of statistics. 1999; p. 94–128.

12. Fritsch FN, Carlson RE. Monotone piecewise cubic interpolation. SIAM Journal on Numerical Analysis. 1980;17(2):238–246.

13. Mayer BT, Krantz EM, Swan D, Ferrenberg J, Simmons K, Selke S, et al. Transient oral human cytomegalovirus infections indicate inefficient viral spread from very few initially infected cells. Journal of virology. 2017;91(12):e00380–17.

14. Gillespie DT. A general method for numerically simulating the stochastic time evolution of coupled chemical reactions. Journal of computational physics. 1976;22(4):403–434.

15. Hobbs TR, Blue SW, Park BS, Greisel JJ, Conn PM, Pau FK. Measurement of blood volume in adult rhesus macaques (Macaca mulatta). Journal of the American Association for Laboratory Animal Science. 2015;54(6):687–693.

16. Yan AW, Cao P, McCaw JM. On the extinction probability in models of within-host infection: the role of latency and immunity. Journal of mathematical biology. 2016;73(4):787–813.

17. Lilleri D, Kabanova A, Revello MG, Percivalle E, Sarasini A, Genini E, et al. Fetal human cytomegalovirus transmission correlates with delayed maternal antibodies to gH/gL/pUL128-130-131 complex during primary infection. PloS one. 2013;8(3):e59863.

18. Picone O, Vauloup-Fellous C, Cordier A, Guitton S, Senat M, Fuchs F, et al. A series of 238 cytomegalovirus primary infections during pregnancy: description and outcome. Prenatal diagnosis. 2013;33(8):751–758.

19. Moström MJ, Scheef EA, Sprehe LM, Szeltner D, Tran D, Hennebold JD, et al. Immune Profile of the Normal Maternal-Fetal Interface in Rhesus Macaques and Its Alteration Following Zika Virus Infection. Frontiers in immunology. 2021; p. 2906.

20. Nigro G, Adler SP, La Torre R, Best AM. Passive immunization during pregnancy for congenital cytomegalovirus infection. New England Journal of Medicine. 2005;353(13):1350–1362.

21. Visentin S, Manara R, Milanese L, Da Roit A, Forner G, Salviato E, et al. Early primary cytomegalovirus infection in pregnancy: maternal hyperimmunoglobulin therapy improves outcomes among infants at 1 year of age. Clinical infectious diseases. 2012;55(4):497–503.

22. Nigro G, Adler SP, Parruti G, Anceschi MM, Coclite E, Pezone I, et al. Immunoglobulin therapy of fetal cytomegalovirus infection occurring in the first half of pregnancy—a case-control study of the outcome in children. Journal of Infectious Diseases. 2012;205(2):215–227.

23. Maidji E, Nigro G, Tabata T, McDonagh S, Nozawa N, Shiboski S, et al. Antibody treatment promotes compensation for human cytomegalovirus-induced pathogenesis and a hypoxia-like condition in placentas with congenital infection. The American journal of pathology. 2010;177(3):1298–1310.

24. Revello MG, Lazzarotto T, Guerra B, Spinillo A, Ferrazzi E, Kustermann A, et al. A randomized trial of hyperimmune globulin to prevent congenital cytomegalovirus. New England Journal of Medicine. 2014;370(14):1316–1326.

25. Renzette N, Gibson L, Bhattacharjee B, Fisher D, Schleiss MR, Jensen JD, et al. Rapid intrahost evolution of human cytomegalovirus is shaped by demography and positive selection. PLoS genetics. 2013;9(9):e1003735.

26. Hughes BL, Clifton RG, Rouse DJ, Saade GR, Dinsmoor MJ, Reddy UM, et al. A trial of hyperimmune globulin to prevent congenital cytomegalovirus infection. New England Journal of Medicine. 2021;385(5):436–444.